Human Molecular Genetics, 2000, Vol. 9, No. 13 **2009–2018**

Polyglutamine length-dependent interaction of Hsp40 and Hsp70 family chaperones with truncated N-terminal huntingtin: their role in suppression of aggregation and cellular toxicity

Nihar Ranjan Jana, Motomasa Tanaka, Guang-hui Wang and Nobuyuki Nukina+

Laboratory for CAG Repeat Diseases, RIKEN Brain Science Institute, 2–1 Hirosawa, Wako-shi, Saitama 351-0198, Japan

Received 18 April 2000; Revised and Accepted 19 June 2000

Huntington's disease (HD) is an autosomal dominant neurodegenerative disorder caused by polyglutamine expansion in the disease protein, huntingtin. In HD patients and transgenic mice, the affected neurons form characteristic ubiquitin-positive nuclear inclusions (NIs). We have established ecdysone-inducible stable mouse Neuro2a cell lines that express truncated N-terminal huntingtin (tNhtt) with different polyglutamine lengths which form both cytoplasmic and nuclear aggregates in a polyglutamine length- and inducer dose-dependent manner. Here we demonstrate that newly synthesized polyglutamine-expanded truncated huntingtin interacts with members of Hsp40 and Hsp70 families of chaperones in a polyglutamine length-dependent manner. Of these interacting chaperones, only Hdj-2 and Hsc70 frequently (Hdj-2 > Hsc70) co-localize with both the aggregates in the cellular model and with the NIs in the brains of HD exon 1 transgenic mice. However, Hdj-2 and Hsc70 do not co-localize with cytoplasmic aggregates in the brains of transgenic mice despite these chaperones being primarily localized in the cytoplasmic compartment. This strongly suggests that the chaperone interaction and their redistribution to the aggregates are two completely different phenomena of the cellular unfolded protein response. This unfolded protein response is also evident from the dramatic induction of Hsp70 on expression of polyglutamine-expanded protein in the cellular model. Transient overexpression of either Hdj-1 or Hsc70 suppresses the aggregate formation; however, suppression efficiency is much higher in Hdj-1 compared with Hsc70. Overexpression of Hdj-1 and Hsc70 is also able to protect cell death caused by polyglutamine-expanded tNhtt and their combination proved to be most effective.

INTRODUCTION

Expansion of CAG triplets within the coding regions of target genes is the cause of several autosomal dominant neurodegenerative diseases including Huntington's disease (HD), several spinocerebellar ataxias (SCAs), dentatorubral pallidoluysian atrophy and X-linked spinal bulbar muscular atrophy (SBMA) (1–3). One of the common characteristic features of all the above diseases is the formation of insoluble aggregates, in particular intranuclear aggregates or nuclear inclusions (NIs) (4–6). The affected neurons in the brains of HD patients show NIs containing N-terminal huntingtin fragments (7–9), and transgenic mice expressing exon 1 of the HD gene containing >115 CAG repeats also have neuronal NIs even before they develop neurological symptoms (10). These findings led us to postulate that such NIs are toxic and responsible for the pathology of HD. In fact, several cellular models of HD also demonstrate that the nuclear aggregates of polyglutamine protein are associated with cell death (11–15). However, two recent studies have raised the possibility that this aggregation may not be the primary factor causing cell death (16,17).

The mechanism that leads the polyglutamine-expanded proteins to aggregate is unknown. One hypothesis is that the glutamine repeats are able to form a polar zipper, an unusual motif for protein–protein interaction (18,19). This polar zipper was predicted to form either between two different molecules with glutamine repeats or within one molecule, forming a hairpin loop. Aggregate formation would then be enhanced by an expanded polyglutamine tract via transglutaminase-catalyzed cross-linking (20) or by aberrant interaction with other proteins dependent on polyglutamine length (21–23). There is also the possibility that the extended polyglutamine tract may destabilize the native conformation of the protein, thereby causing the protein to misfold and aggregate. The fact that the NIs are ubiquitinated raises the possibility that the polyglutamine-expanded proteins become misfolded, with protein degrading machinery such as proteasomes being affected. Indeed recent reports suggest that NIs in SCA1 (24), SCA3 (25,26) and SBMA (27) co-localize with chaperone Hdj-2 and proteasome components. Furthermore, overexpression of the chaperone suppressed the aggregate formation in those studies.

+To whom correspondence should be addressed. Tel: +81 48 467 9702; Fax: +81 48 462 4796; Email: nukina@brain.riken.go.jp

Correct protein folding is an essential biological process, and for correct folding in the cellular milieu, many proteins interact with molecular chaperones. The heat shock protein 70 (Hsp70) class of molecular chaperones is thought to bind early in the folding process to the extended conformation of a polypeptide chain with a preference for hydrophobic sequences, and to maintain the polypeptide in a soluble conformation (28,29). ATP binding and hydrolysis on Hsp70 are coupled to substrate binding and release by conformational changes in the chaperone that represent cooperation between the substrate binding and ATPase domains of Hsp70 (30,31). To facilitate protein folding, Hsp70 must interact with a co-chaperone protein that regulates its ATPase activity (32–34). A major class of Hsp70 co-chaperone proteins is the Hsp40 family. These chaperones also bind to a misfolded substrate and are capable of initiating refolding and of preventing aggregation without the help of Hsp70 (35). On release from the chaperone, a polypeptide may either fold to its native conformation or enter into the degradation machinery of the cells. Chaperones may also play an active role in directing misfolded or mutant proteins to proteolysis by ubiquitin–proteasome pathways (36,37).

In the present study, we hypothesized that the polyglutamine-expanded huntingtin protein is probably misfolded and that the cellular chaperone system may be affected. Therefore, we investigated the involvement of various chaperones in the pathogenesis of HD using HD exon 1 transgenic mice and an inducible stable mouse Neuro2a cell line that expresses truncated N-terminal huntingtin (tNhtt) containing different polyglutamine lengths. We demonstrate that several chaperones of the Hsp family interact with newly synthesized tNhtt in a polyglutamine length-dependent manner and that some chaperones are also co-localized with the aggregates. We further show that the transient overexpression of some of these chaperones reduces the aggregate formation as well as cellular toxicity caused by expanded polyglutamine tracts.

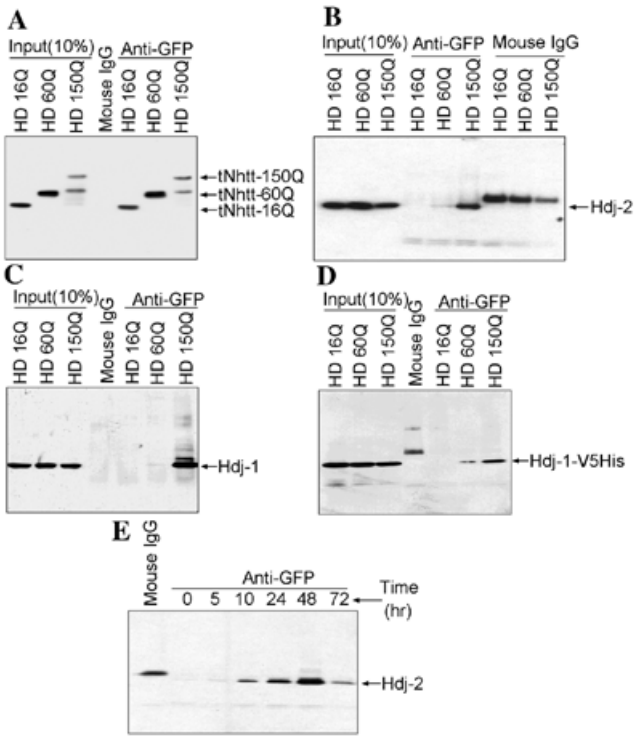

Figure 1. Polyglutamine length-dependent co-immunoprecipitation of Hdj-2 and Hdj-1 chaperones with tNhtt. HD 16Q-23, 60Q-14 and 150Q-28 cell lines were differentiated with 5 mM dbcAMP and induced with 1 μM ponasterone A for 2 days. The total cell lysate was immunoprecipitated with anti-GFP and the immunoprecipitated materials were analyzed by immunoblotting. Blots were sequentially probed with huntingtin (**A**), Hdj-2 (**B**) and Hdj-1 (**C**) antibody. (**D**) The above-mentioned cell lines were transfected with Hdj-1 expression plasmids and, 24 h after transfection, cells were treated with dbcAMP and ponasterone A for another 24 h and then total cell lysate was processed for immunoprecipitation by anti-GFP. The blot was probed with V5 antibody. (**E**) Differentiated HD 150Q-28 cells were induced for different time periods and the total cell lysate processed for immunoprecipitation by anti-GFP. Protein on the blot was detected with anti-Hdj-2.

RESULTS

Interaction of Hsp40 and Hsp70 chaperone families with polyglutamine-expanded tNhtt

We have established stable and inducible mouse Neuro2a cell lines that express tNhtt with enhanced green fluorescent protein (EGFP) containing 16, 60 and 150 glutamine residues. These cell lines are denoted HD 16Q-23, 60Q-14 and 150Q-28 and the expressed proteins are tNhtt-16Q, -60Q and -150Q, respectively. Using this cellular model, we showed that the formation of aggregates and cell death induced by tNhtt were polyglutamine length- and inducer dose-dependent (38). In the present study, we used these cell lines to examine the interaction of various chaperones with normal and polyglutamine-expanded tNhtt. Each cell line was differentiated with N^6,2-*O*-dibutyryl-cAMP (dbcAMP) and induced with ponasterone A for 2 days and then the total cell lysate prepared for immunoprecipitation by anti-green fluorescent protein (anti-GFP). The immunoprecipitates were analyzed by SDS–PAGE and immunoblotting. The blots were first probed with either anti-huntingtin or anti-GFP to confirm the immunoprecipitation of GFP–huntingtin protein with various glutamine repeats (Fig. 1A). Both anti-GFP and anti-huntingtin detected two major bands in HD 150Q-28 cell lysate because of the instability of the longer CAG repeats which was further confirmed by PCR analysis. The blots were then sequentially probed with different chaperone antibodies. Figure 1 shows the polyglutamine length-dependent co-immunoprecipitation of Hdj-1 and Hdj-2 chaperones. Both Hdj-2 (Fig. 1B) and Hdj-1 (Fig. 1C) precipitated well with tNhtt-150Q, very poorly with tNhtt-60Q, but did not precipitate at all with tNHtt-16Q. The interaction of Hdj-1 was further confirmed by transient transfection of the HD 16Q-23, 60Q-14 and 150Q-28 cells with Hdj-1 expression plasmid, immunoprecipitation by anti-GFP antibody and detection by V5-tag antibody (Fig. 1D). Control experiments containing mouse IgG instead of anti-GFP antibody resulted in no precipitation of the chaperones. In the reverse experiments using both anti-Hdj-1 and anti-Hdj-2 antibodies, we also observed co-immunoprecipitation of tNhtt-150Q with Hdj-1 and Hdj-2 (data not shown). In another experiment, differentiated HD 150Q-28 cells were induced for different time periods (from 5 h to 3 days) and the cells collected at each time-point then processed for immunoprecipitation with anti-GFP antibody. A blot of the precipitated proteins was then probed with anti-Hdj-2 antibody. The result

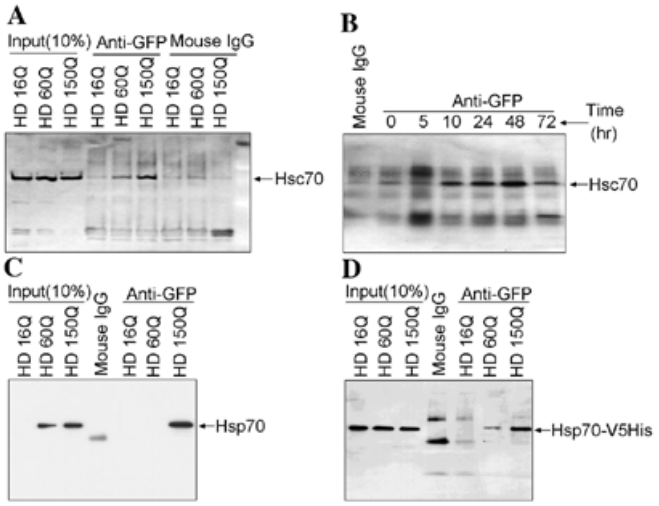

Figure 2. Co-immunoprecipitation of Hsc70 and Hsp70 chaperones with the polyglutamine-expanded tNhtt. (**A**, **B** and **C**) Cells were treated and processed for immunoprecipitation as described in Figure 1B, E and C, respectively. Blots were probed with either anti-Hsc70 (A and B) or anti-Hsp70 (C). (**D**) HD 150Q-28 cells were transfected with Hsp70 expression plasmids. Total cell lysate was processed for immunoprecipitation and protein was detected with V5 antibody.

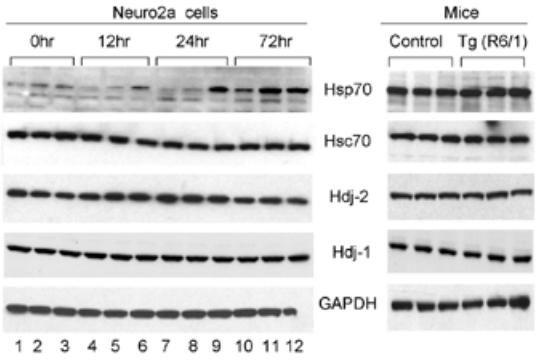

Figure 3. Effect of expanded-polyglutamine protein on expression levels of various chaperones. Differentiated HD 16Q-23, 60Q-14 and 150Q-28 cell lines were induced with 1 μM ponasterone A for different time periods and then the total cell lysate was analyzed by immunoblotting. Equal amounts of protein (20 μg) were loaded in each lane. Lanes 1, 4, 7 and 10, cell lysate expressing tNhtt-16Q; lanes 2, 5, 8 and 11, cell lysate expressing tNhtt-60Q; lanes 3, 6, 9 and 12, cell lysate expressing tNhtt-150Q. Brains from 30- to 36-week-old transgenic mice and age-matched controls were used.

shows that the immunoprecipitated Hdj-2 due to newly synthesized tNhtt-150Q was detected from 10 h onwards and increased steadily up to 2 days (Fig. 1E). The amount of immunoprecipitated Hdj-2 decreased on the third day due to a gradual increase in aggregate formation of the soluble protein.

Figure 2A and C demonstrate similar polyglutamine length-dependent co-immunoprecipitation of Hsc70 and Hsp70 chaperones with tNhtt. Reverse experiments were also carried out to confirm the results (data not shown). Interactions of Hsp70 (Fig. 2D) and Hsc70 (data not shown) were further confirmed by transfecting cells with their respective expression plasmids, immunoprecipitating with anti-GFP antibody and probing a blot with V5 antibody. Figure 2B shows the time dependency of the immunoprecipitatable Hsc70. Several other chaperones, namely Hsp27, Hsp60, Hsp90α and Hsp104, were tested in similar co-immunoprecipitation experiments, but none was immunoprecipitated by anti-GFP antibody.

Expanded polyglutamine protein elicits stress response

Surprisingly, during the immunoprecipitation experiment we observed a very high level of induction of Hsp70 in HD 60Q-14 and 150Q-28 cells. Consequently, we examined the expression levels of various other interacting chaperones in cells induced for different time periods as well as in transgenic mice (R6/1 line) with age-matched controls. In the cellular system, although Hsp70 was normally undetectable, its expression was dramatically up-regulated in a polyglutamine length-dependent manner (Fig. 3). However, the expression levels of various other chaperones, namely Hdj-1, Hdj-2 and Hsc70, did not change. No differences in the expression levels of any of the chaperones were observed between control and transgenic mice (Fig. 3). In both control and transgenic mice, Hsp70 was normally expressed at quite high levels and did not show any further increase in transgenic mice until 30–35 weeks when the mice began to display severe HD symptoms.

Co-localization of Hdj-2 and Hsc70 chaperones with the polyglutamine aggregates in the cellular model

Since the chaperones interacted with the soluble form of polyglutamine-expanded tNhtt, we next examined whether the aggregated form also contained those chaperones. Therefore, we performed immunocytochemical staining of those chaperones. In wild-type Neuro2a cells or HD 16Q-28, 60Q-14 and 150Q-28 cells, endogenous Hdj-2 and Hsc70 were primarily localized in the cytoplasmic compartment with very faint nuclear staining. However, on induction of the mutant protein in HD 60Q-14 or 150Q-28 cells these chaperones redistributed to the aggregates and showed co-localization with GFP aggregates (Fig. 4). The staining pattern of Hsc70 in the aggregates was much weaker and the frequency of the Hsc70 positively stained aggregates were also comparatively lower than Hdj-2. However, we were unable to find any Hdj-1- and Hsp70-positive aggregates in either HD 60Q-14 or 150Q-28 cells, although both interacted with the polyglutamine-expanded protein.

Redistribution of Hdj-2 and Hsc70 chaperones to the NIs in HD exon 1 transgenic mice

We next examined the subcellular localization of various chaperones in the brains of HD exon 1 transgenic mice. On immunostaining of the R6/1 transgenic mice brain sections, we found localization of Hdj-2 and Hsc70 chaperones to the NIs (Fig. 5). In control mice, these chaperones were mainly localized to the cytoplasm. A quantitative estimation of the ubiquitin-, Hdj-2- and Hsc70-positive NIs in the cerebral cortex and striatum area is shown in Figure 2B. Immunofluorescence staining was performed to visualize the respective positively stained fluorescein isothiocyanate (FITC)-labeled NIs, and nuclei were counterstained with propidium iodide. The brains of R6/1 transgenic mice at 10–12 weeks contained

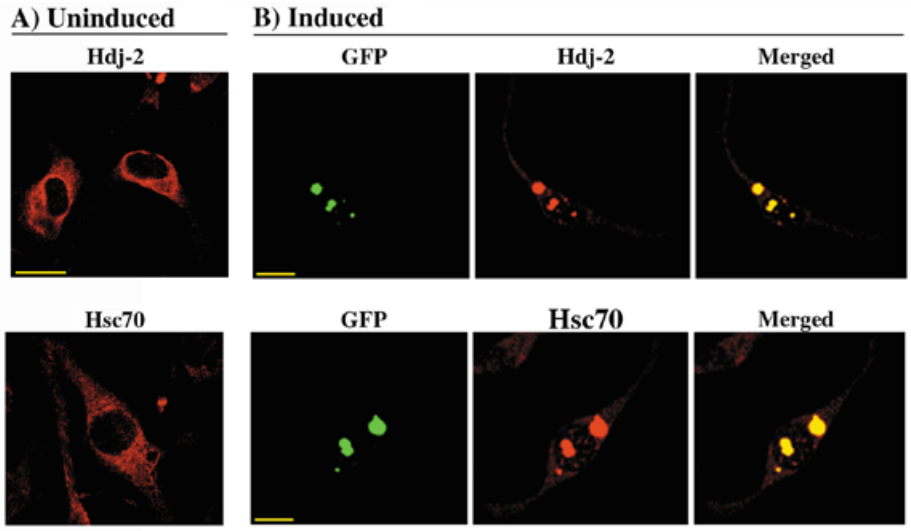

Figure 4. Localization of Hdj-2 and Hsc70 chaperones in the polyglutamine aggregates. Differentiated HD 150Q-28 cells were left untreated (**A**) or treated with ponasterone A (**B**) for 2 days and then cells were processed for immunofluorescence staining. Cy3-conjugated (red) secondary antibody was used to label either Hdj-2 or Hsc70. Merging (yellow) of the two signals (red and green) illustrates co-localization. Scale bars: (A) 20 µm; (B, top) 20 µm; (B, bottom) 10 µm.

~17% of ubiquitin-positive NIs, which increased to 72% at 30–35 weeks. However, Hdj-2- and Hsc70-positive NIs were undetectable at 10–12 weeks and detectable to 51 and 25%, respectively, at 30–35 weeks. In 10- to 12-week-old R6/2 mice, the percentage of ubiquitin-, Hdj-2- and Hsc70-positive NIs were relatively higher than in 30- to 35-week-old R6/1 mice. The frequency of Hdj-2- and Hsc70-positive NIs were much lower compared with that of ubiquitin-positive NIs, and the frequency of Hsc70-positive NIs was ~50% lower than that of Hdj-2-positive NIs in both transgenic mice. Hdj-1 and Hsp70 did not localize to the NIs in both transgenic mice. Figure 6 demonstrates immunofluorescence double labeling of the Hdj-2 chaperone and ubiquitin in transgenic mouse brain sections. Anti-ubiquitin positively stained nuclear and many cytoplasmic aggregates. However, anti-Hdj-2 antibody mostly stained the nuclear aggregates. A similar phenomenon was observed in the case of Hsc70. Several other Hsps, i.e. Hsp27, Hsp60, Hsp90α and Hsp105, did not localize to the NIs.

Suppression of polyglutamine protein aggregation by Hdj-1 and Hsc70 chaperones

Next we examined whether the interaction of the chaperone with polyglutamine-expanded tNhtt was trying to keep the polyglutamine protein in a soluble form or whether it was enhancing the process of aggregation. We addressed this problem by overexpressing those chaperones into the HD 150Q-28 cells. Overexpression of Hdj-1 efficiently prevented aggregate formation in HD 150Q-28 cells (Fig. 7A). Hsc70 overexpression (Fig. 7B) also had a significant effect on aggregate suppression; however, Hsp70 (Fig. 7C) had no effect. Co-expression of either Hsc70 or Hsp70 with Hdj-1 did not improve the suppressive effect that was observed with over-expression of Hdj-1 alone. The J-domain deleted form of Hdj-1 or ATPase domain deletion mutant of Hsc70 also had a significant effect on suppression of aggregate formation (Fig. 7A and B). However, overexpression of only the J-domain of Hdj-1 or only the ATPase domain of Hsc70 had no effect. The J-domain deletion mutant of Hdj-1 or ATPase domain deletion mutant of Hsc70 both retain their capacity to bind with the polyglutamine-expanded tNhtt as evidenced from immuno-precipitation (data not shown). A similar suppressive effect of Hdj-1 and Hsc70 on polyglutamine protein aggregation was also observed in HD 60Q-14 cell lines. We further confirmed our result by transiently transfecting those chaperones along with pIND-tNhtt-EGFP-150Q at different ratios into Neuro2a cells stably expressing VgRXR (the functional ecdysone receptor). Twenty-four hours after transfection, cells were induced with ponasterone A (1 µM) and, at 48 h post-transfection, cells were fixed and processed for immuno-fluorescence staining of Hdj-1 and Hsc70 by V5 antibody. As shown in Figure 8, either Hdj-1 or Hsc70 along with poly-glutamine-expanded huntingtin efficiently prevent aggregate formation and counting of the aggregates (Fig. 8D) in the trans-fected cells revealed a dramatic extent of aggregate suppression.

Hdj-1 and Hsc70 chaperones protect against cell death caused by expanded polyglutamine protein

The ability of the Hdj-1 and Hsc70 chaperones to suppress aggregate formation prompted us to investigate the change in cellular toxicity caused by polyglutamine-expanded tNhtt. We used HD 150Q-28 cells for this investigation. On induction with 1 µM ponasterone A, the differentiated HD 150Q-28 cells showed ~22–36% death on the third and fourth days. Over-expression of Hdj-1 significantly protected against this cell death. Hsc70 also showed a small suppressive effect on cellular toxicity but this was not statistically significant. Co-expression of Hsc70 with Hdj-1 improved the protective effect further in comparison with Hdj-1 alone (Fig. 9A). The expression levels of Hdj-1, Hsc70 and tNhtt-150Q are shown in Figure 9B.

DISCUSSION

Protein aggregation is the most common characteristic feature among the polyglutamine diseases. The mechanism that causes

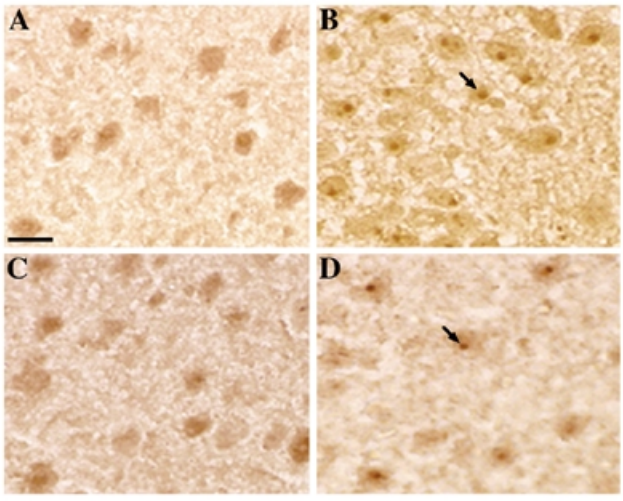

E

Ubiquitin and chaperones	Positively stained NI (%)		
	R6/1 (10-12 weeks)	R6/1 (30-35 weeks)	R6/2 (10-12 weeks)
Ubiquitin	17 ± 6	72 ± 12	86 ±15
Hdj-2	Nil	51 ± 8	65 ± 7
Hsc70	Nil	25 ± 8	34 ± 5

Figure 5. Co-localization of Hdj-2 and Hsc70 chaperones to the NIs in the brains of HD exon 1 transgenic mice. Brain sections from control and transgenic 30- to 36-week-old mice of were used for immunohistochemical staining. (**A**) Control mouse brain stained with anti-Hdj-2 antibody. (**B**) Transgenic mouse (R6/1) brain stained with anti-Hdj-2 antibody. (**C**) Control mouse brain stained with anti-Hsc70 antibody. (**D**) Transgenic mouse (R6/1) brain stained with anti-Hsc70 antibody. Scale bars, 50 µm. (**E**) Quantification of ubiquitin-, Hdj-2- and Hsc70-positive NIs in the R6/1 and R6/2 lines of HD exon 1 transgenic mice. Positively stained NIs were estimated by counting ~500 propidium iodide-stained nuclei in different parts of the cerebral cortex and striatum using three transgenic mice of each age group. Values are means ± SD.

polyglutamine-expanded proteins to aggregate is not fully understood. Here, we demonstrate that several chaperones of the Hsp family interact with polyglutamine-expanded protein in a glutamine repeat length-dependent manner. This suggests that polyglutamine-expanded proteins are misfolded and become prone to aggregation and that the misfolding propensity is directly proportional to the length of the glutamine repeats. Among several chaperones tested, the members of the Hsp40 (Hdj-1 and Hdj-2) and Hsp70 (both constitutive and inducible form) families bind to the polyglutamine-expanded proteins.

Of these four interacting chaperones, Hdj-2 and Hsc70 were frequently co-localized with the aggregates in both the cellular and HD exon 1 transgenic mouse model, indicating that their interaction might be involved in enhancing the process of aggregation. The hypothesis was further supported by the fact that the yeast chaperone Hsp104 has been shown to be necessary for the conversion of prions from soluble to insoluble form through the stabilization of certain folding intermediates. This phenomenon was lost when Hsp104 was overexpressed or removed from the system (39,40). However, in both our cellular and transgenic mouse models, the staining pattern of Hsc70 in the aggregates was very weak and the frequency of positively stained aggregates was also quite low compared with that of Hdj-2. Furthermore, immunofluorescence double labeling between Hdj-2 and ubiquitin in the transgenic mouse brain section revealed that the Hdj-2 associated with only nuclear and not cytoplasmic aggregates. This indicates that Hdj-2 and Hsc70 are most likely not involved in the aggregation process, since these chaperones are mostly cytoplasmic, and if their interaction helps polyglutamine proteins to aggregate we would expect at least some cytoplasmic aggregates to be positively stained for these chaperones.

One possible explanation as to why the chaperones bind to the nuclear aggregates follows. The polyglutamine-expanded proteins escape from the cytoplasmic chaperone barrier, gradually accumulate and form aggregates inside the nucleus. When the aggregates are sufficiently large, a stress response is induced. As a result, the chaperone targets the nuclear aggregates but eventually the attempt is unsuccessful. Alternatively, the chaperones might help the expanded polyglutamine protein to enter the nucleus, where the chaperone-bound polyglutamine protein complex associates with the neighboring molecules and forms aggregates. The nuclear environment possibly favors the aggregation process because the nucleus is less efficient than the cytoplasm in refolding or degrading misfolded proteins (16,41,42). From our observations, it is conceivable that the chaperone interaction with the soluble form of polyglutamine-expanded proteins and their

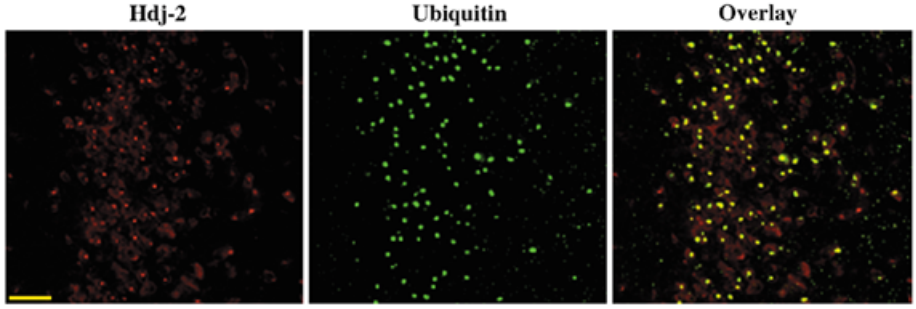

Figure 6. Immunofluorescence double labeling of ubiquitin and Hdj-2 in the NI. Brain sections from 30- to 36-week-old transgenic mice (R6/1) was used. Brain section was incubated with anti-Hdj-2 (anti-mouse) and anti-ubiquitin (anti-rabbit) antibodies and then labeled with anti-rabbit FITC-conjugated and anti-mouse Cy3-conjugated antibodies. (**A**) Hdj-2 (red). (**B**) Ubiquitin (green). (**C**) Overlay of the two signals (yellow). Scale bar, 50 µm.

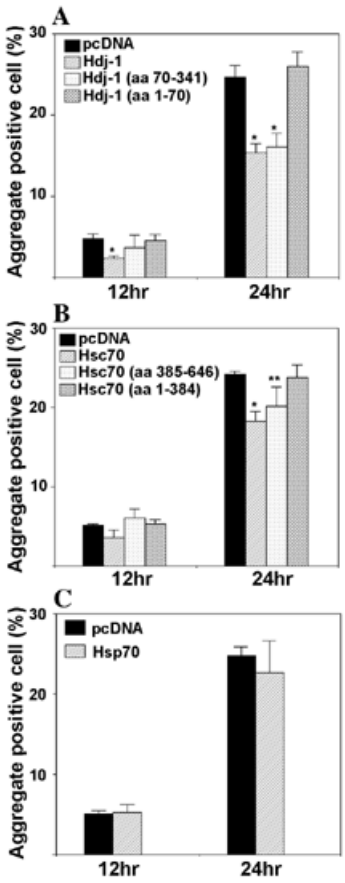

Figure 7. Effect of overexpression of various chaperones on polyglutamine protein aggregation. HD 150Q-28 cells were transfected with empty pcDNA or Hdj-1, Hsc70 or Hsp70 expression vector. After 24 h, cells were re-plated in the chamber slides and, after another 24 h, cells were differentiated (5 mM dbcAMP) and induced (100 nM ponasterone A) simultaneously. Aggregate formation was monitored at 12 and 24 h post-induction. (**A**) Effect of overexpression of full-length or various deletion mutants of Hdj-1. (**B**) Effect of overexpression of full-length and various deletion mutants of Hsc70. (**C**) Effect of overexpression of Hsp70. Values are means ± SEM; $n = 4$. $^*P < 0.001$; $^*P < 0.01$, compared with respective empty pcDNA-transfected experiment with respect to time.

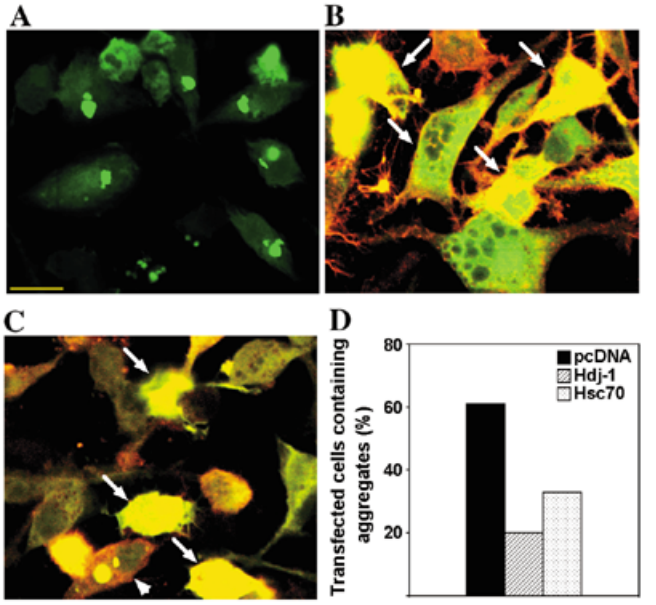

Figure 8. Immunofluorescence demonstration of the prevention of polyglutamine protein aggregation in cells overexpressing either Hdj-1 or Hsc70 chaperones. Neuro2a cells stably expressing VgRXR were transfected with either Hdj-1 or Hsc70 (2 µg each) along with pIND-tNhtt-EGFP-150Q (0.5 µg) and, 24 h after transfection, cells were induced with 1 µM ponasterone A. Twenty-four hours post-induction, cells were processed for immunofluorescence staining of Hdj-1 and Hsc70. Cy3-conjugated secondary antibody was used to label the Hdj-1 and Hsc70. (**A**) Cells transfected with pIND-tNhtt-EGFP-150Q and an empty pcDNA vector. (**B**) Cells transfected with Hdj-1 and pIND-tNhtt-EGFP-150Q. Arrows indicate cells expressing both Hdj-1 and tNhtt-150Q. (**C**) Cells transfected with Hsc70 and pIND-tNhtt-EGFP-150Q. Arrows indicate cells expressing both Hsc70 and tNhtt-150Q. The arrowhead indicates the cell containing aggregates. (**D**) Quantification of the number of aggregates in the cells that overexpressed Hdj-1 and Hsc70 chaperones. Scale bar, 20 µm.

recruitment to the polyglutamine aggregates are two completely different phenomena of the cellular unfolded protein response.

The co-localization of Hdj-2 chaperone to the NIs has been demonstrated in SCA1 (24), SCA3 (26) and SBMA (27) and in all the disease models examined overexpression of Hdj-2 chaperone suppresses aggregate formation. Co-localization of Hdj-1 and Hsp70 with the NIs and suppression of aggregate formation by Hdj-1 has also been demonstrated in SCA3 (26). In the cellular model of HD used in the present study, we found suppression of aggregate formation by Hdj-1 and Hsc70. This strongly suggests that the common target of Hsp40 and Hsp70 family members are any polyglutamine-expanded protein and that Hsp40 and Hsp70 are effective in the suppression of polyglutamine-mediated protein aggregation. However, the suppression efficiency differs among the members of these two families of chaperones. Our results suggest that Hsp40 family members are much more effective in aggregation suppression compared with members of the Hsp70 family. Whether these differences also exist among the members of the same family has yet to be determined.

The Hsp40 family chaperones are known to be co-chaperones for the Hsp70 family and modulate the cellular protein folding by binding to misfolded polypeptides via the C-terminal domain and regulating the ATPase activity of the Hsp70 family members through the N-terminal J-domain (33,34). However, there are reports that the members of the Hsp40 family are also capable of refolding the misfolded substrates and preventing aggregation without the help of Hsp70 family members (35,43). The fact that the J-domain deletion mutant of Hdj-1 still suppresses the aggregate formation strongly suggests that the Hsp40 family chaperones can work alone and also possibly in cooperation with the Hsp70 family to suppress aggregation. How those chaperones are involved in the folding process of unfolded polyglutamine-expanded protein is not clear. Possibly, at higher concentrations, the chaperone-bound folding intermediate efficiently prevents the intra- and intermolecular polar zipper formation and keeps the polyglutamine protein in a soluble form while enhancing their degradation by ubiquitin–proteasome pathways at the same time. The Hsp40 and Hsp70 families of chaperones have been shown to play a critical role in the rapid

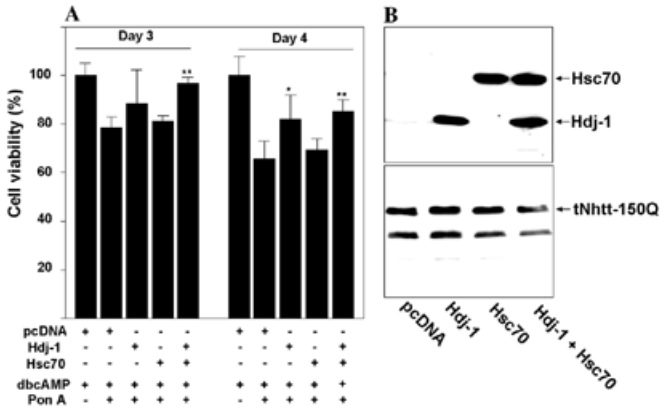

Figure 9. Reduction of polyglutamine-mediated cellular toxicity on overexpression of Hdj-1 and Hsc70 chaperones. HD 150Q-28 cells were transfected with empty vector (pcDNA) or plasmids encoding Hdj-1 or Hsc70. After 24 h, cells were re-plated to the 96-well plates, differentiated (5 mM dbcAMP) and induced (1 μM ponasterone A) simultaneously. Cell viability was measured by MTT assay and monitored at the third and fourth days of induction. Values are the means ± SEM; $n = 12$. $^{*}P < 0.01$; $^{**}P < 0.001$, compared with pcDNA-transfected and ponasterone A-treated experiment. (**B**) Expression levels of various transfected chaperones and tNhtt-150Q detected at 48 h post-transfection. Twenty-four hours after transfection, cells were differentiated and induced as indicated above. Chaperones on the blot were detected by ECL with 30 s exposure and tNhtt-150Q was detected with 1 min exposure.

degradation of misfolded proteins by the ubiquitin–proteasome pathway (36,37).

Another interesting observation in the present study was the polyglutamine length-dependent induction of Hsp70 in the cellular model, despite being unable to detect any major changes in Hsp70 levels in the HD exon 1 transgenic mice (R6/1) until 30–35 weeks, when they showed severe HD symptoms. The induction of Hsp70 has also been reported in the cellular model of SCA3 but not in their transgenic model (26). Many stressful conditions induce Hsp70, which increases the cell's tolerance to stress. Induction of Hsp70 by polyglutamine-expanded protein suggests that the cell is under stress and trying to compensate. However, the factors generating this stress are currently unknown. One possibility is that the utilization and redistribution of chaperones as well as proteasomes (unpublished data) to the aggregates creates a deficit in their normal active cellular pool, which in turn increases the accumulation of misfolded proteins and ultimately creates stress. Our hypothesis is supported by the observation that inhibition of proteasome function leads to the induction of various chaperones (44). Moreover, the cellular deficit of chaperones and proteasomes might ultimately result in disease progression by disturbing vital cellular function.

In the present study, we found that overexpression of the Hsp40 family chaperones significantly reduces the cellular toxicity created by polyglutamine-expanded tNhtt. This protective effect was further improved by overexpressing Hsp40 with Hsc70. Recently, overexpression of the Hsp40 chaperone has also been reported to suppress the cell death due to mutant SCA3 protein (26). Moreover, an *in vivo* study in a *Drosophila* SCA3 disease model demonstrated that overexpression of Hsp70 suppresses polyglutamine-induced neurodegeneration and delays the progression of the disease without a visible effect on NI formation (45). In the cellular model of SCA3, Hsp70 overexpression does not have a suppressive effect on aggregate formation (26). In the cellular model for HD, we were unable to detect any significant suppression of aggregate formation or cellular toxicity on Hsp70 overexpression. One possible explanation is that in cellular models, endogenous Hsp70 is highly induced by polyglutamine-expanded protein and therefore further overexpression does not make a further difference. However, the specificity of Hsp70 protection against polyglutamine protein-mediated cell death remains to be explained, since Hsp70 itself is anti-apoptotic and can rescue the cell from stress-induced apoptosis (46,47).

The challenge is to determine whether the Hsp40 and Hsp70 family chaperones really suppress the aggregation and protect the neurodegeneration in the *in vivo* HD transgenic mouse model. If so, and if there are no adverse effects of overexpression, then these chaperones may prove to be effective therapeutic molecules by which to slow the progression of HD and also other polyglutamine diseases.

MATERIALS AND METHODS

Mice

Heterozygous HD exon 1 transgenic male mice of R6/1 (115 CAG repeats) and R6/2 (145 CAG repeats) lines were obtained from the Jackson Laboratory (Bar Harbor, ME) (Jackson codes: B6CBA-TgN [Hdexon1]61 and B6CBA-TgN[Hdexon1]62) and maintained by crossing carrier males with CBA females. The genotyping and CAG repeat sizing was carried out using a PCR assay and Genescan, respectively, as described previously (48). Mice (transgenic and their age-matched controls) were sacrificed using ether anesthesia, and their brains carefully removed and collected in Tissue-Tek (Sakura Finetek, Tokyo, Japan), frozen with powdered solid CO_2 and stored at –80°C.

Antibodies

Antibodies utilized in this study were purchased from the following sources. The rabbit polyclonal anti-Hdj-1 (SPA-400) and mouse monoclonal anti-Hsp70 (SPA-810) were purchased from StressGen Biotechnologies (Victoria, British Columbia). Mouse monoclonal anti-Hdj-2 (MS-225) was from Neomarkers (Union City, CA). Goat polyclonal anti-Hsc70 (sc-1059), goat polyclonal anti-Hsp60 (sc-1052), rabbit polyclonal anti-Hsp105 (sc-1805), goat polyclonal anti-Hsp90α and goat polyclonal anti-Hsp27 (sc1798) were from Santa Cruz Biotechnology (Santa Cruz, CA). Mouse monoclonal anti-GAPDH (MAB374) was from Chemicon International (Tenecula, CA). Rabbit polyclonal anti-huntingtin (corresponding to N-terminal amino acid sequences) was raised in our laboratory. Goat anti-rabbit IgG–Cy3, goat anti-mouse IgG–Cy3 and donkey anti-goat IgG–Cy3 (Molecular Probes, Eugene, OR) were utilized as secondary antibodies in indirect immunofluorescence. Horseradish peroxidase (HRP)-conjugated anti-mouse IgG and anti-rabbit IgG (Amersham Life Science, Little Chalfont, UK) and anti-goat IgG (Santa Cruz Biotechnology) were utilized as secondary antibodies in immunoblotting.

Expression plasmids

The tNhtt expression constructs pIND-tNhtt-EGFP-16Q, pIND-tNhtt-EGFP-60Q and pIND-tNhtt-EGFP-150Q have been described previously (39). Each construct contains 1–90 amino acids of tNhtt with a different polyglutamine length fused to the N-terminus of EGFP. The Hsp70 and Hsp40 expression vectors in pcDNA3.1/GS were obtained from Invitrogen (Carlsbad, CA). The full-length Hsc70 cDNA was isolated from human brain total RNA by using RT–PCR. Primer sequences were 5′-GTGGCTTCCTTCGTTATTGG-3′ (sense) and 5′-TTAATCAACCTCTTCAATGGTGGG-3′ (antisense). Proof reading polymerase (TaKaRa, Kyoto, Japan) was used in the PCR reaction. PCR fragments were A-tailed and ligated into pGEM-T Easy Vector (Promega, Madison, WI) and confirmed by sequencing. The full-length, ATPase domain (amino acids 1–384) and the ATPase domain deletion (amino acids 385–646) mutant of Hsc70 expression vector in pcDNA6/V5-His were prepared using PCR and subcloning the product in frame into the *Kpn*I–*Xho*I site of the vector. The primer sequences were: 5′-ACGGGGTACCATGGCCAAGGGACCTGCAC-3′ (sense, for full-length and ATPase domain mutant); 5′-ACGGGGTACCATGGTGTCTGGAGACAAGTC-3′ (sense, for ATPase domain deletion mutant); 5′-ACCGCTCGAGCGGATCAACCTCTTCAATGG-3′ (antisense for full-length and ATPase domain deletion mutant); and 5′-ACCGCTCGAGGGCTGCCTGGACAGCTGCACCATAAGC-3′ (antisense for ATPase domain mutant). The J-domain mutant (amino acids 1–70) or J-domains deletion (amino acids 70–341) mutant of Hdj-1 was also constructed from full-length Hdj-1 by subcloning the PCR product into the *Bam*HI–*Xho*I site of the pcDNA6/V5-His plasmid. Primer sequences were: 5′-ACGCGGATCCACCATGGGTAAAGACTACTACCA-3′ (sense for J-domain mutant); 5′-ACCGCTCGAGTTCCTCCCCGTAGCGGTCGA-3′ (antisense for J-domain mutant); 5′-ACGCGGATCCACCATGGGCCTAAAGGGGAGTGGCC-3′ (sense for J-domain deletion mutant); and 5′-ACCGCTCGAGATATATTGGAAGAACCTGCT-3′ (antisense for J-domain deletion mutant). Underlined sequences represent the sites for restriction enzymes.

Cell culture and treatments

Mouse Neuro2a cells stably expressing tNhtt-EGFP-16Q, tNhtt-EGFP-60Q and tNhtt-EGFP-150Q were regularly maintained in Dulbecco's modified Eagle's medium (Life Technologies, Gaithersburg, MD) supplemented with 10% fetal bovine serum, 0.4 mg/ml zeocin and 0.4 mg/ml G418. Establishment of stable cell lines has been described earlier (39). Cells were differentiated by treating 5 mM dbcAMP (N^6,2′-*O*-dibutyryladenosine-3′:5′-cyclic monophosphate sodium salt (Nacalai Tesque, Kyoto, Japan) and induced with different concentrations (0.1–2 μM) of ponasterone A (Invitrogen).

Co-immunoprecipitation experiments

Cells were washed with cold phosphate-buffered saline (PBS), scraped, pelleted by centrifugation and lysed on ice for 30 min with RIPA buffer (10 mM HEPES pH 7.4, 150 mM NaCl, 10 mM EDTA, 2.5 mM EGTA, 1% Triton X-100, 0.1% SDS, 1% sodium deoxycholate, 10 mM NaF, 5 mM $Na_4P_2O_7$, 0.1 mM Na_3VO_4, 1 mM PMSF, 0.1 mg/ml Aprotinin). Cell lysate was briefly sonicated, centrifuged for 10 min at 15 000 *g* at 4°C and the supernatants (total soluble extract) were used for immunoprecipitation. Protein concentration was measured according to the method of Bradford using Bio-Rad protein assay reagent (Bio-Rad, Hercules, CA) and bovine serum albumin as a standard. For each immunoprecipitation experiment, 200 μg of protein in 0.2 ml of RIPA buffer was incubated either with 5 μl (2 μg) of anti-GFP antibody or 4 μl (2 μg) of normal mouse IgG. After 5–6 h of incubation at 4°C with rotation, 10 μl of magnetic protein G beads (Perspective Biosystems, Framingham, MA) were added and incubation was continued at 4°C overnight. The beads were pulled down with a magnet (Dynal, Oslo, Norway) and washed six times with RIPA buffer. Bound proteins were eluted from the beads with SDS (1×) sample buffer, vortexed, boiled for 5 min and analyzed by immunoblotting.

Immunoblotting

The total cell lysate, mouse brain total soluble extracts (homogenate after centrifugation at 15 000 *g* for 10 min) or the immunoprecipitated proteins were separated through SDS–polyacrylamide gel (7.5–20%) electrophoresis and transferred onto PVDF membrane (Immobilon-P; Millipore, Bedford, MA). The membranes were successively incubated in blocking buffer [5% skim milk in TBST (50 mM Tris pH 7.5, 0.15 M NaCl, 0.05% Tween)], with primary antibody in TBST, and then with secondary antibody conjugated with HRP in TBST. Detection was carried out with enhanced chemiluminescence (ECL) reagent (Amersham Life Science).

Immunofluorescence techniques

Cells grown in chamber slides were differentiated and induced together for 2 days. Cells were washed twice with PBS, fixed with 4% paraformaldehyde in PBS for 20 min, permeabilized with 0.5% Triton X-100 in PBS for 5 min, washed extensively and then blocked with 5% non-fat dried milk in TBST for 1 h. Primary antibody incubation was carried out overnight at 4°C. After several washings with TBST, cells were incubated with appropriate secondary antibody for 1 h, washed several times and mounted in antifade solution (Vectashield Mounting Media; Vector, Burlingame, CA). The primary antibodies, anti-Hdj-2 and anti-Hdj-1, were used at 1:1000 dilution and anti-Hsc70, anti-Hsp70, anti-Hsp60, anti-Hsp105 and anti-Hsp90α were used at 1:250 dilution. Secondary antibodies conjugated with Cy3 were used at 1:1000 dilution. Samples were observed using a confocal microscope (Fluoview; Olympus, Tokyo, Japan) and digital images were assembled using Adobe Photoshop. For immunofluorescence staining of various chaperones and ubiquitin in the transgenic mouse brain sections, the sections were fixed and incubated with different primary antibody in a similar manner to that described for the immunohistochemistry. The appropriate FITC- or Cy3-conjugated secondary antibody was used to visualize the expression and localization. In some experiments, nuclei were counterstained with propidium iodide.

Immunohistochemistry

The frozen brains mounted on Tissue-Tek were sectioned in freezing microtome to 20 μm thickness. Sections were fixed with 4% paraformaldehyde in PBS for 20 min, washed several

times, blocked with 5% non-fat dried milk for 1 h and then incubated overnight with primary antibody. Staining was carried out using ABC Elite kit (Vector). Briefly, after primary antibody incubation, sections were washed and incubated for 1 h at room temperature with the appropriate biotinylated secondary antibody, washed, incubated with ABC reagent, washed, exposed for several minutes to DAB substrate, washed, dehydrated, cleared and mounted. Dilutions of the different primary antibodies used were the same as described for immunofluorescence.

Transfections, quantitation of aggregate formation and cell viability

Transfection of various chaperones (2 μg/well each) was carried out in 60 mm tissue cultured plates using Lipofectamine 2000 (Life Technologies) according to the manufacturer's instructions. Twenty-four hours after transfection, cells were collected, counted by Trypan blue and re-plated into the chamber slides (for counting aggregation) or 96-well tissue cultured plates (for cell viability assay). Forty-eight hours post-transfection, cells were treated with dbcAMP and ponasterone A. For counting aggregation, 1×10^3 cells were seeded into each well of the chamber slides and, for cell viability assay, 5×10^3 cells were seeded into each well of 96-well plates. Both aggregate formation and cell viability were monitored at different time-points. Aggregate formation was manually counted under a fluorescence microscope and the cells containing more than one aggregate were considered to have a single aggregate. Cell viability was determined using the 3-(4,5-dimethylthiazol-2-yl)-2,5-diphenyl tetrazolium bromide (MTT) assay described previously (39). Statistical analysis was performed using paired *t*-test, with $P < 0.05$ considered statistically significant.

In other experiments, we transiently transfected 0.5 μg of pIND-tNhtt-EGFP-150Q along with different concentrations of various chaperones (0.5–2 μg) into mouse Neuro2a cells stably transfected with pVgRXR which express a functional ecdysone receptor. Twenty-four hours after transfection, cells were differentiated with 5 mM dbcAMP and induced with 1 μM of ponasterone A. At 24 h post-transfection, cells were processed for immunofluorescence staining of Hdj-1 and Hsc70 using V5 antibody. The appropriate Cy3-conjugated secondary antibody was used to visualize the transfected cells. The number of aggregates was counted using ~100 transfected cells for quantitative estimation.

ACKNOWLEDGEMENT

This work was supported partly by a grant from the Ministry of Health and Welfare.

REFERENCES

1. Ross, C.A. (1995) When more is less: pathogenesis of glutamine repeats neurodegenerative diseases. *Neuron*, **15**, 493–496.
2. Paulson, H.L. and Fischbeck, K.H. (1996) Trinucleotide repeats in neurogenetic disorders. *Ann. Rev. Neurosci.*, **19**, 79–107.
3. Reddy, P.S. and Housman, D.E. (1997) The complex pathology of trinucleotide repeats. *Curr. Opin. Cell. Biol.*, **9**, 364–372.
4. Ross, C.A. (1997) Intranuclear neuronal inclusions: a common pathogenic mechanism of glutamine-repeat neurodegenerative diseases? *Neuron*, **19**, 1147–1150.
5. Kim, T.W. and Tanzi, R.E. (1998) Neuronal intranuclear inclusions in polyglutamine diseases: nuclear weapons or nuclear fallout? *Neuron*, **21**, 657–659.
6. Paulson, H.L. (1999) Protein fate in neurodegenerative proteinopathies: polyglutamine diseases join the misfold. *Am. J. Hum. Genet.*, **64**, 339–345.
7. DiFiglia, M., Sapp, E., Chase, K.O., Davies, S.W., Bates, G.P., Vonsattel, J.P. and Aronin, N. (1997) Aggregation of huntingtin in neuronal intranuclear inclusions and dystrophic neurites in brain. *Science*, **277**, 1990–1993.
8. Becher, M.W., Kotzuk, J.A., Sharp, A.H., Davies, S.W., Bates, G.P., Price, D.L. and Ross, C.A. (1998) Intranuclear neuronal inclusions in Huntington's disease and dentatorubral and pallidoluysian atrophy: correlation between the density of inclusions and IT15 CAG triplet repeat length. *Neurobiol. Dis.*, **4**, 387–397.
9. Gutekunst, C.A., Li, S.H., Yi, H., Mulroy, J.S., Kuemmerle, S., Jones, R., Rye, D., Ferrante, R.J., Hersch, S.M. and Li, X.J. (1999) Nuclear and neuropil aggregates in Huntington's disease: relationship to neuropathology. *J. Neurosci.*, **19**, 2522–2534.
10. Davies, S.W., Turmaine, M., Cozens, B.A., DiFiglia, M., Sharp, A.H., Ross, C.A., Scherzinger, E., Wanker, E.E., Mangiarini, L. and Bates, G.P. (1997) Formation of neuronal intranuclear inclusions underlines the neurological disfunction in mice transgenic for HD mutation. *Cell*, **90**, 537–548.
11. Cooper, J.K., Schilling, G., Peters, M.F., Herring, W.J., Sharp, A.H., Kaminsky, Z., Masone, J., Khan, F.A., Delanoy, M., Borchelt, D.R. *et al.* (1998) Truncated N-terminal fragments of huntingtin with expanded glutamine repeats form nuclear and cytoplasmic aggregates in cell culture. *Hum. Mol. Genet.*, **7**, 783–790.
12. Martindale, D., Hackam, A., Wieczorek, A., Ellerby, L., Wellington, C., McCutcheon, K., Singaraja, R., Kazemi-Esfarjani, P., Devon, R., Kim, S.U. *et al.* (1998) Length of huntingtin and its polyglutamine tract influences localization and frequency of intranuclear aggregates. *Nature Genet.*, **18**, 150–154.
13. Hackam, A.S., Singaraja, R., Zhang, T., Gan, L. and Hayden, M.R. (1999) *In vitro* evidence for both the nucleus and cytoplasm as subcellular sites of pathogenesis in Huntington's disease. *Hum. Mol. Genet.*, **8**, 25–33.
14. Moulder, K.L., Onodera, O., Burke, J.R., Strittmatter, W.J. and Johnson Jr, E.M. (1999) Generation of neuronal intranuclear inclusions by polyglutamine-GFP: analysis of inclusion clearance and toxicity as a function of polyglutamine length. *J. Neurosci.*, **19**, 705–715.
15. Li, S.-H., Cheng, A.L., Li, H. and Li, X.-J. (1999) Cellular defects and altered gene expression in PC12 cells stably expressing mutant huntingtin. *J. Neurosci.*, **19**, 5159–5172.
16. Klement, I.A., Skinner, P.J., Kaytor, M.D., Yi, H., Hersch, S.M., Clark, H.B., Zoghbi, H.Y. and Orr, H.T. (1998) Ataxin-1 nuclear localization and aggregation: role in polyglutamine-induced disease in *SCA1* transgenic mice. *Cell*, **95**, 41–53.
17. Saudou, F., Finkbeiner, S., Devys, D. and Greenberg, M.E. (1998) Huntingtin acts in the nucleus to induce apoptosis but death does not correlate with the formation of intranuclear inclusions. *Cell*, **95**, 55–66.
18. Perutz, M.F., Johnson, T., Suzuki, M. and Finch, J.T. (1994) Glutamine repeats as polar zippers: their possible role in inherited neurodegenerative diseases. *Proc. Natl Acad. Sci USA*, **91**, 5355–5358.
19. Stott, K., Blackburn, J.M., Butler, P.J.G. and Perutz, M. (1995) Incorporation of glutamine repeats makes protein oligomerize: implications for neurodegenerative diseases. *Proc. Natl Acad. Sci. USA*, **92**, 6509–6513.
20. Kahlem, P., Terre, C., Green, H. and Djian, P. (1996) Peptides containing glutamine repeats as substrates for transglutaminase-catalyzed cross-linking: relevance to diseases of the nervous system. *Proc. Natl Acad. Sci. USA*, **93**,14580–14585.
21. Sittler, A., Walter, S., Wedemeyer, N., Hasenbank, R., Scherzinger, E., Eickhoff, H., Bates, G.P., Lehrach, H. and Wanker, E.E. (1998) SH3GL3 associates with the huntingtin exon-1 protein and promotes the formation of polygln-containing protein aggregates. *Mol. Cell.*, **2**, 427–436.
22. Li, X.-J., Li, S.-H., Sharp, A.H., Nucifora, F.C., Schilling, G., Lanahan, A., Worley, P., Snyder, S.H. and Ross, C.A (1995) A huntingtin associated protein enriched in brain with implications for pathology. *Nature*, **378**, 398–402.
23. Faber, P.W., Barnes, G.T., Srinidhi, J., Chen, J., Gusella, J.F. and MacDonald, M.E. (1998) Huntingtin interacts with a family of WW domain proteins. *Hum. Mol. Genet.*, **7**, 1463–1474.
24. Cummings, C.J., Mancini, M.A., Antalffy, B., DeFranco, D.B., Orr, H.T. and Zoghbi, H.Y. (1998) Chaperone suppression of aggregation and

altered subcellular proteasome localization imply protein misfolding in *SCA1*. *Nature Genet.*, **19**, 148–154.
25. Chai, Y., Koppenhafer, S.L., Shoesmith, S.J., Perez, M.K. and Paulson, H.L. (1999) Evidence for proteasome involvement in polyglutamine disease: localization to nuclear inclusions in SCA3/MJD and supression of polyglutamine aggregation *in vitro*. *Hum. Mol. Genet.*, **8**, 673–682.
26. Chai, Y., Koppenhafer, S.L., Bonini, N.M. and Paulson, H.L. (1999) Analysis of the role of heat shock protein (hsp) molecular chaperones in polyglutamine disease. *J. Neurosci.*, **19**, 10338–10347.
27. Stenoien, D.L., Cummings, C.J., Adams, H.P., Mancini, M.G., Patel, K., DeMartino, G.N., Marcelli, M., Weigel, N.L. and Mancini M.A. (1999) Polyglutamine-expanded androgen receptors form aggregates that sequester heat shock proteins, proteasome components and SRC-1, and are suppressed by the HDJ-2 chaperone. *Hum. Mol. Genet.*, **8**, 731–741.
28. Landry, S.J., Jordan, R., McMacken, R. and Gierasch, L.M. (1992) Different conformations for the same polypeptide bound to chaperones DnaK and GroEL. *Nature*, **355**, 455–457.
29. Blond-Elguindi, S., Cwirla, S.E., Dower, W.J., Lipshutz, R.J., Sprang, S.R., Sambrook, J.F. and Gething, M.J. (1993) Affinity panning of a library of peptides displayed on bacteriophages reveals the binding specificity of BiP. *Cell*, **75**, 717–728.
30. Kamath-Loeb, A.S., Lu, C.Z., Suh, W.C., Lonetto, M.A. and Gross, C.A. (1995) Analysis of three DnaK mutant proteins suggests that progression through the ATPase cycle requires conformational changes. *J. Biol. Chem.*, **270**, 30051–30059.
31. Fung, K.L., Hilgenberg, L., Wang, N.M. and Chirico, W.J. (1996) Conformations of the nucleotide and polypeptide binding domains of a cytosolic Hsp70 molecular chaperone are coupled. *J. Biol. Chem.*, **271**, 21559–21565.
32. Cyr, D.M. (1997) The Hsp40 (DnaJ related) family of proteins. In Gething, M.J. (ed.), *Guidebook to Molecular Chaperones and Protein Folding Factors*. Oxford University Press, Oxford, UK, pp. 89–95.
33. Hartl, F.U. (1996) Molecular chaperones in cellular protein folding. *Nature*, **381**, 571–580.
34. Hendricks, J.P. and Hartl, F.U. (1993) Molecular chaperone functions of heat shock proteins. *Annu. Rev. Biochem.*, **62**, 349–384.
35. Lu, Z. and Cyr, D.M. (1998) The conserved carboxyl terminus and zinc finger-like domain of the co-chaperone Ydj1 assist Hsp70 in protein folding. *J. Biol. Chem.*, **273**, 5970–5978.
36. Lee, D.H., Sherman, M.Y. and Goldberg, A.L. (1996) Involvement of molecular chaperone Ydj1 in the ubiquitin-dependent degradation of short-lived and abnormal proteins in *Saccharomyces cerevisiae*. *Mol. Cell. Biol.*, **16**, 4773–4781.
37. Bercovich, B., Stancovsky, I., Mayer, A., Blumenfeld, N., Laszlo, A., Schwartz, A.L. and Ciechanover, A. (1997) Ubiquitin-dependent degradation of certain protein substrates *in vitro* requires the molecular chaperone Hsc70. *J. Biol. Chem.*, **272**, 9002–9010.
38. Wang, G.H., Mitsui, K., Kotliarova, S., Yamashita, A., Nagao, Y., Tokuhiro, S., Iwatsubo, T., Kanazawa, I. and Nukina, N. (1999) Caspase activation during apoptotic cell death induced by expanded polyglutamine in N2a cells. *Neuroreport*, **10**, 2435–2438.
39. Chernoff, Y.O., Lindquist, S.L., Ono, B., Inge-Vechtomov, S.G. and Liebman, S.W. (1995) Role of the chaperone protein Hsp104 in propagation of the yeast prion-like factor [psi+]. *Science*, **268**, 880–884.
40. DebBurman, S.K., Raymond, G.J., Caughey, B. and Lindsquit, S.L. (1997) Chaperone-supervised conversion of prion protein to its protease-resistant form. *Proc. Natl Acad. Sci.*, **94**, 13938–13943.
41. Perez, M.K., Paulson, H.L., Pendse, S.J., Saionz, S.J., Bonini, N.M. and Pittman, R.N. (1998). Recruitment and the role of nuclear localization in polyglutamine-mediated aggregation. *J. Cell Biol.*, **143**, 1457–1470.
42. Michels, A.A., Kanon, B., Konings, A.W.T., Ohtsuka, K., Bensaude, O. and Kampinga, H.H. (1997) Hsp70 and Hsp40 chaperone activities in the cytoplasm and the nucleus of mammalian cells. *J. Biol. Chem.*, **272**, 33283–33289.
43. Meacham, G.C., Lu, Z., King, S., Sorscher, E., Tousson, A. and Cyr, D.M. (1999) The Hdj-2/Hsc70 chaperone pair facilitates early step in CFTR biogenesis. *EMBO J.*, **18**, 1492–1505.
44. Bush, K.T., Goldberg, A.L. and Nigam, S.K. (1997) Proteasome inhibition leads to a heat-shock response, induction of endoplasmic reticulum chaperones and thermotolerance. *J. Biol. Chem.*, **272**, 9086–9092.
45. Warrick, J.M., Chan, H.Y.E., Gray-Board, G.L., Chai, Y., Paulson, H.L. and Bonini, N.M. (1999) Suppression of polyglutamine-mediated neurodegeneration in *Drosophila* by the molecular chaperone Hsp70. *Nature Genet.*, **23**, 425–428.
46. Jaattela, M., Wissing, D., Kokholm, K., Kallunki, T. and Egeblad, M. (1998) Hsp70 exerts its anti-apoptotic function downstream of caspase-3-like proteases. *EMBO J.*, **17**, 6124–6134.
47. Mosser, D.D., Caron, A.W., Bourget, L., Denis-Larose, C. and Massie, B. (1997) Role of the human heat shock protein hsp70 in protection against stress-induced apoptosis. *Mol. Cell. Biol.*, **17**, 5317–5327.
48. Mangiarini, L. Sathasivam, K., Seller, M., Cozens, B., Harper, A., Hetherington, C., Lawton, M., Trottier, Y., Lehrach, H., Davies, S.W. and Bates, G.P. (1996) Exon-1 of the HD gene with an expanded CAG repeat is sufficient to cause a progressive neurological phenotype in transgenic mice. *Cell*, **87**, 493–506.